Macromolecular Bioscience
www.mbs-journal.de

A Cerberus-Inspired Anti-Infective Multicomponent Gatekeeper Hydrogel against Infections with the Emerging "Superbug" Yeast *Candida auris*

*Dennis Kubiczek, Carolin Flaig, Heinz Raber, Steffen Dietz, Ann-Kathrin Kissmann, Thomas Heerde, Nicholas Bodenberger, Andreas Wittgens, Melaine González-Garcia, Fan Kang, Octavio L. Franco, Ludger Staendker, Anselmo J. Otero-González, Paul Walther, Kay E. Gottschalk, Tanja Weil, and Frank Rosenau**

The pathogenic yeast *Candida auris* has received increasing attention due to its ability to cause fatal infections, its resistance toward important fungicides, and its ability to persist on surfaces including medical devices in hospitals. To brace health care systems for this considerable risk, alternative therapeutic approaches such as antifungal peptides are urgently needed. In clinical wound care, a significant focus has been directed toward novel surgical (wound) dressings as first defense lines against *C. auris*. Inspired by Cerberus the Greek mythological "hound of Hades" that prevents the living from entering and the dead from leaving hell, the preparation of a gatekeeper hybrid hydrogel is reported featuring lectin-mediated high-affinity immobilization of *C. auris* cells from a collagen gel as a model substratum in combination with a release of an antifungal peptide drug to kill the trapped cells. The vision is an efficient and safe two-layer medical composite hydrogel for the treatment of severe wound infections that typically occur in hospitals. Providing this new armament to the repertoire of possibilities for wound care in critical (intensive care) units may open new routes to shield and defend patients from infections and clinical facilities from spreading and invasion of *C. auris* and probably other fungal pathogens.

1. Introduction

The yeast *Candida auris* is a relatively new pathogen that was first isolated in 2009 from a Japanese patient.[1] It causes severe invasive infections in hospitalized patients, which lead to high mortality rates between 35% and 60%.[2,3] Resistance against fungicides such as polyenes and azoles imposes an additional threat[4] and transmission between patients and the environment can lead to a spread of the pathogen also in care units.[5] Therefore, the Centers for Disease Control and Prevention released a clinical alert in June 2016,[6] initiating a broad public discourse, identifying *C. auris* as an emerging "superbug."[7] As conventional treatments with antifungal drugs fail due to the multidrug resistance of *C. auris*, antimicrobial peptides (AMP) can be regarded as promising alternative fungicides. AMPs reduce structural integrity

Dr. D. Kubiczek, C. Flaig, H. Raber, S. Dietz, A.-K. Kissmann, T. Heerde, Dr. F. Rosenau
Institute of Pharmaceutical Biotechnology
Ulm University
Ulm 89081, Germany
E-mail: frank.rosenau@uni-ulm.de

Dr. N. Bodenberger, Dr. A. Wittgens, Prof. T. Weil, Dr. F. Rosenau
Synthesis of macromolecules
Max-Planck Institute for Polymer Research
Mainz 55128, Germany

M. González-Garcia, Prof. A. J. Otero-González
Center for Protein Studies
Havana University
Havana 10200, Cuba

The ORCID identification number(s) for the author(s) of this article can be found under https://doi.org/10.1002/mabi.202000005.

F. Kang, Prof. K. E. Gottschalk
Institute of Experimental Physics
Ulm University
Ulm 89081, Germany

Prof. O. L. Franco
Center for Biochemical and Proteomics Analyses
Catholic University of Brasilia
Brasilia 70040-00, Brazil

Prof. O. L. Franco
Department of Biotechnology
Catholic University Dom Bosco
Campo Grande 79117-010, Brazil

Dr. L. Staendker
Core Facility Functional Peptidomics
Ulm University Hospital
Ulm 89081, Germany

Prof. P. Walther
Central Facility for Electron Microscopy
Ulm University
Ulm 89081, Germany

DOI: 10.1002/mabi.202000005

of the cell walls of these pathogens by physical disintegration and/or pore formation and they are expected to provide treatment options even against organisms resistance to conventional antifungal drugs that typically address distinct target structure (e.g., surface proteins, enzymes, etc.).[8,9] However, the therapeutic potential of AMPs has been limited by their considerable toxicities also toward human cells.[10] The AMP Cm-p5 derived from a peptide isolated from the coastal mollusk *Cenchritis muricatus* represents an exception as the AMP exhibited efficient antifungal activity against *C. albicans*, *C. parapsilosis*, *Cryptococcus neoformans*, and *Trichophyton rubrum* with only negligible toxicity toward mammalian cells.[11,12] Therefore, Cm-p5 provides an attractive therapeutic index opening various opportunities for developing efficient and safe antifungal drugs also against *C. auris* infections, such as wound protections after initial contamination.[12] In order to receive effective AMP drugs for applications in wound care, there is an urgent demand to deliver these peptides to the wound or site of infection in a safe and convenient manner. Hydrogels have been recognized as material of choice for wound dressings, since they are optimal regulators of moisture and can create positive environments for wound healing.[13,14] As so-called "active" dressings, functional hydrogels are produced and marketed supplying additional features beyond simple moisture control to further support and improve the healing process. Next-generation hydrogels promote regeneration of damaged tissues, they serve as efficient anti-infectives against multidrug-resistant pathogens,[15] or they also allow monitoring of the healing process.[13] AMPs have been loaded into hydrogels for topical applications[16,17] on the wound surface at the infection site and to achieve first line of defense against fatal wound infections, for example, for applications in intensive care units and after surgery of contaminated patients. The mannose-specific lectin B (LecB) as a tetrameric protein providing four binding sites toward sugar residues on the surface of bacteria and higher cells[18,19] has already been used to bind and immobilize carbapenem-resistant *Pseudomonas aeruginosa* within a hydrogel matrix that were subsequently eradicated by the respective AMPs.[15]

Inspired by *Cerberus*, the three-headed gatekeeper dog of the underworld Hades in the Greek mythology, which prevented souls from migration into the Hades or out of it, we have developed a multicomponent sandwich hydrogel matrix consisting of a protein hydrogel acting as a carrier subsequently coated with LecB for quantitative immobilization of *C. auris* cells creating a dedicated affinity layer on the surface of the carrier hydrogel. The second hydrogel layer consists of a fibrillary hydrogel serving as a reservoir for the anti-*Candida* peptide, Cm-p5, to allow effective elimination of this emerging pathogenic yeast after its binding to the affinity layer. Amino acid-based fibrillary hydrogels, such as the Fmoc-Met-OH hydrogel, are ideally suited because gelation occurs under gentle and physiological conditions by self-assembly instead of chemical cross-linking and thus without undesired covalent and irreversible immobilization of the peptide,[20] although covalent attachment to a surface has been described as a technology to realize antimicrobial coatings.[21] Our system is composed of two different hydrogel layers in the millimeter range of thickness (3.5 mm); however, including the LecB coating as an affinity layer, it comprises three functionalities: 1) a drug reservoir for storage of AMP and 2) a stabilizing carrier layer including the surface affinity layer for immobilization of the pathogen. We envision an efficient and safe hydrogel treatment against severe wound infections often observed in hospitals that are safe, convenient, and efficient to use against pathogens where currently no medication exists.

2. Results and Discussion

2.1. Multicomponent Hydrogel

The two-layer sandwich hydrogel matrix was composed of a bovine serum albumin (BSA)-based protein hydrogel and a second layer consisted of fibrillary hydrogel made from methionine, which is protected by fluorenylmethyloxycarbonyl protection group (Fmoc-Met-OH) (**Figure 1**A).

2.1.1. Drug Reservoir Layer

The Fmoc-Met-OH hydrogel on the other hand was prepared by spontaneous fibril formation by self-assembly upon mixing Fmoc-Met-OH solution in dimethyl sulfoxide (DMSO) with phosphate-buffered saline (PBS) containing the desired concentrations of Cm-p5 as an AMP[20,22] (Figure 1A, "drug reservoir layer"). The dilution lowers the DMSO concentration to 12.5% v/v and thus below toxicological concentration since DMSO is regarded as pharmaceutically active at concentrations between 60% and 90% for topical application.[23] The sandwich resulting from these two different hydrogels can simply be formed by either precasting the Fmoc-Met-OH hydrogel and overlaying it with the protein hydrogel or vice versa mediated by its self-adhesive properties.

2.1.2. Carrier Layer Including the Affinity Layer

The protein hydrogel linker tetrakis-(hydroxymethyl)phosphonium-chloride (THPC) has been suggested in a three-step reaction mechanism via formation of formaldehyde,[24] an amine-formaldehyde reaction to yield an immonium ion in a Mannich-type reaction, and its final coupling by the phosphorus immonium ion reaction (Figure 1A, "hydrogel carrier layer"). After the preparation of the two layers, the affinity layer was created by maleimide cross-linker-mediated decoration of the carrier layer with LecB (YFP-LecB) (Figure 1A, "affinity layer"). To gain full functionality, the AMP Cm-p5 (Figure 1B) as the pharmacological active compound was included during the self-assembly process of the Fmoc-Met-OH reservoir layer. The macroscopic and microscopic structure of the resulting material was analyzed (**Figure 2**A–C).

2.2. Characterization of the Multicomponent Hydrogel

The curve progression during BSA/THPC hydrogel gelation time appeared to be significantly different from that of a typical one-step cross-linking reaction. As THPC exposes four reactive

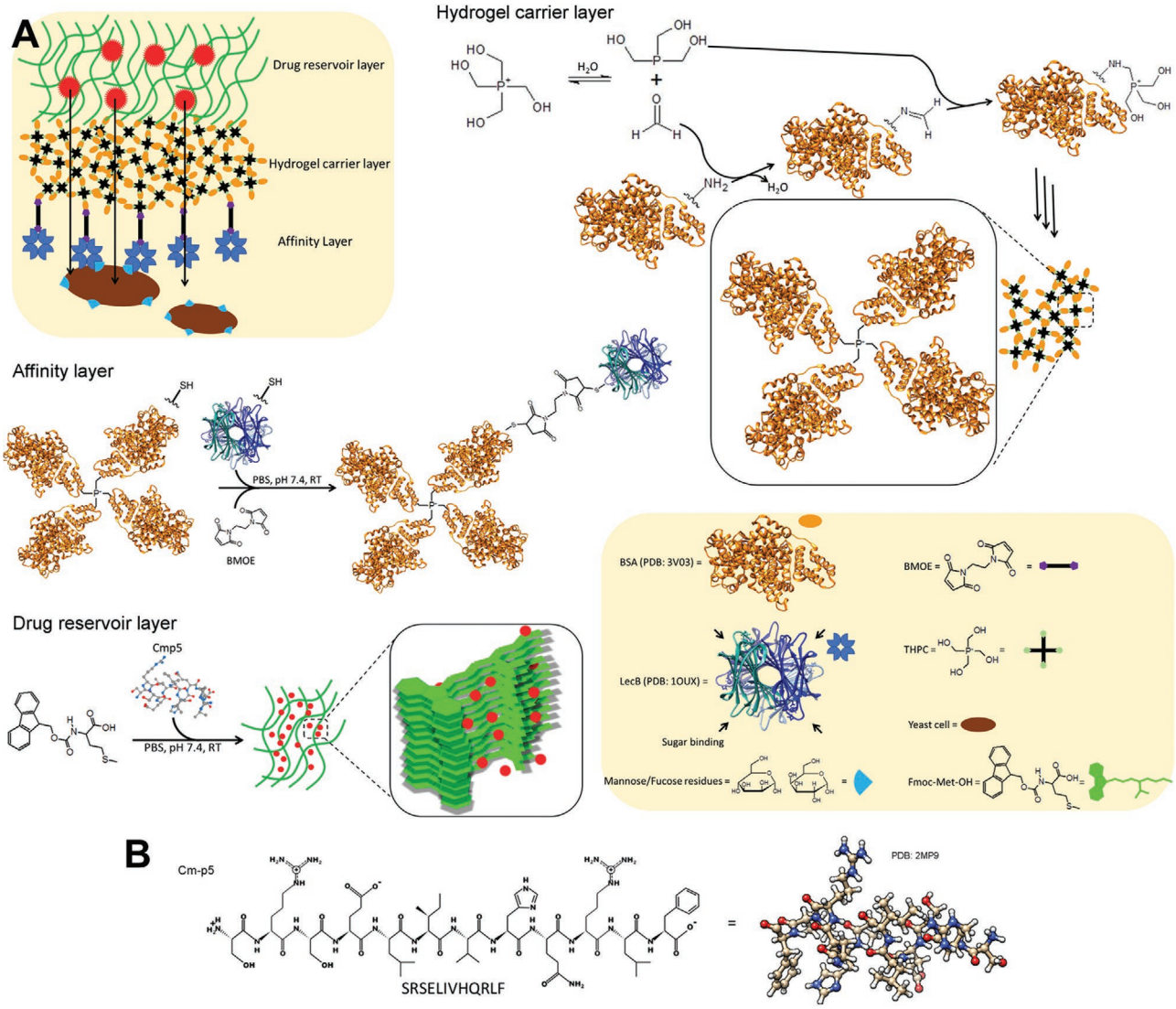

Figure 1. Preparation of BSA/THPC-Fmoc-Met-OH composite hydrogels. A) Protein hydrogel was prepared from BSA by cross-linking with the four-armed amino-reactive THPC. THPC has been suggested in a three-step reaction mechanism via formation of formaldehyde, an amine-formaldehyde reaction to yield an immonium ion in a Mannich-type reaction, and its final coupling through the phosphorus immonium ion reaction. The second hydrogel layer was prepared from Fmoc-protected methionine (Fmoc-Met-OH) by immediate dilution of Fmoc-Met-OH stock solution in DMSO into PBS containing Cm-p5 as an AMP. The protein hydrogel layer was decorated with lectin B by adding thiol-specific maleimide cross-linker bismaleimidoethane (BMOE). B) chemical structure of Cm-p5 (left) and ball-stick representation of its 3D structure derived from PDB:2MP9.

groups,[24] the cross-linking appears to takes place as a reaction of higher order involving at least four major steps, explaining the complex progression of the measured storage and loss moduli. Nevertheless, the BSA/THPC hydrogel thereby reached a manageable stability after around 50 min, although the cross-linking was still not complete (Figure 2D). A linear fit of data after 79 min indicated that the cross-linking was still in progress with 2.85 Pa s^{-1} after this timepoint. For this reason, hydrogels used for the two-layer hydrogel system were prepared at least 16 h before their usage to assure fully cross-linked hydrogel systems of high stability and reproducibility. Gel formation of the fibrillary Fmoc-Met-OH hydrogel proceeds via noncovalent interactions,[22] during dilution of the monomeric compound dissolved in pure DMSO into phosphate-buffered saline (PBS). Gel formation occurs instantaneously by self-assembly, reaching a stable maximum within 5 min (Figure 2E).

The BSA/THPC hydrogel showed the highest storage modulus under these conditions and remained stable until a shear strain of 43.6% (as determined from the crossover points of the loss modulus and the storage modulus, not shown). The Fmoc-Met-OH hydrogel itself, however, revealed a lower storage modulus and remained stable until a shear strain of 5%. As expected, the sandwich of the two layers of hydrogels showed a storage modulus intermediate to its individual components, respectively, and remained stable until a shear strain of 6.4% (Figure 2F), which is in the range of human skin, muscle tissue, or wound dressings based on bacterial cellulose.[25–27] These findings were also supported by cryo scanning electron microscopy. The

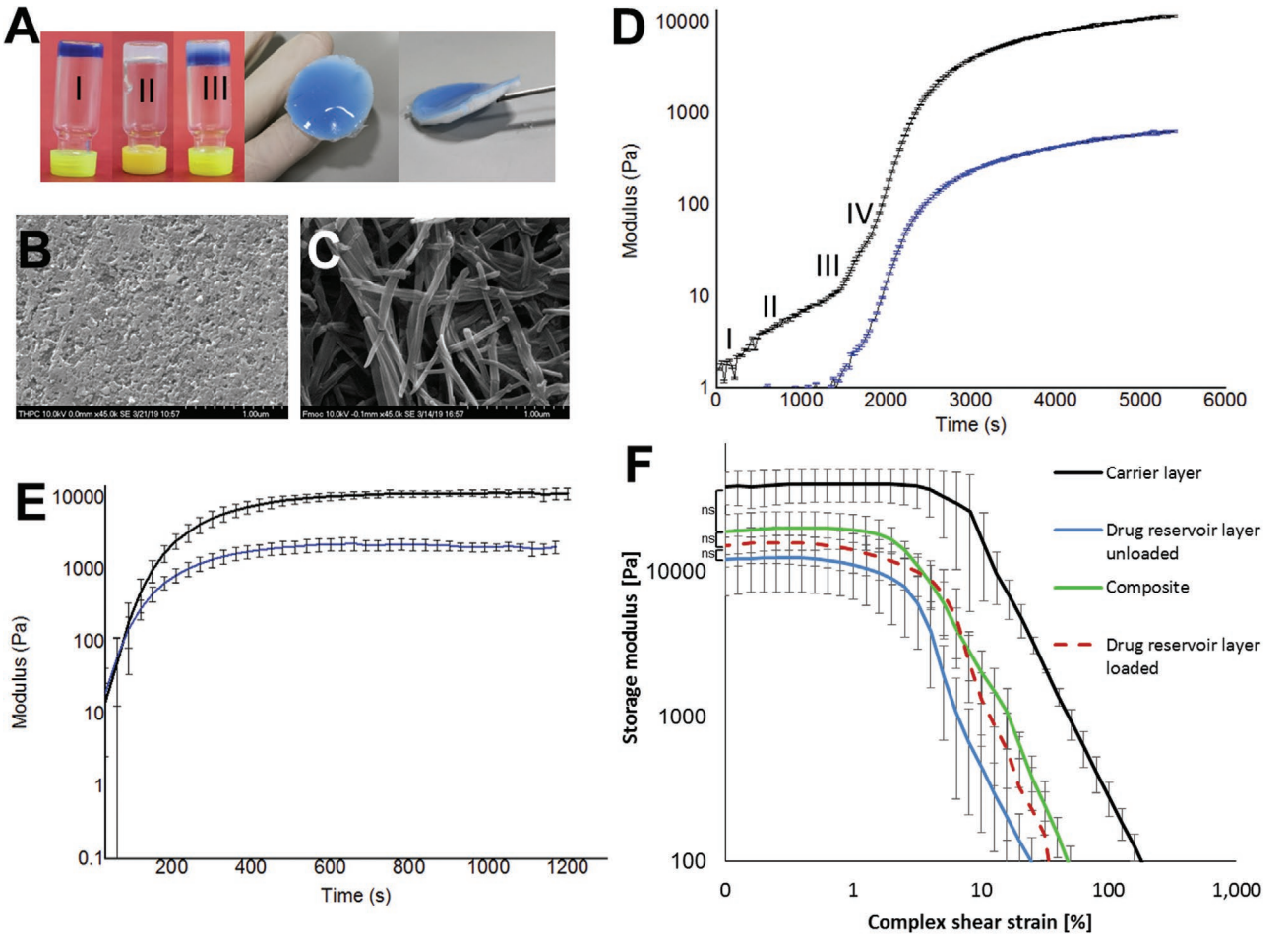

Figure 2. Characterization of the composite hydrogel systems. A) Polymerization was visualized by the vial inversion assay of the carrier layer (I) alone, drug reservoir layer alone (II), and subsequent casting of I onto II (III). The carrier layer was stained with bromophenol blue for better visibility. Patches of the hydrogel sandwich have a diameter of 2.3 cm and a thickness of 3.5 mm. Cryo-scanning electron microscopy of the individual composite material layers reveals a porous structure for the B) BSA/THPC-hydrogel and a fibrillary structure for the C) Fmoc-Met-OH hydrogel. Rheological characterization of the composite hydrogel systems: D) Polymerization of a BSA/THPC hydrogel (carrier layer) monitored through the increase of elastic shear modulus; blue color denotes the loss modulus (G″), whereas black color denotes the storage modulus (G′). E) Polymerization of an Fmoc-Met-OH hydrogel (drug reservoir layer) monitored through the increase of elastic shear modulus, blue color denotes the loss modulus (G″), whereas black color denotes the storage modulus (G′). F) Comparison of elastic shear moduli of BSA/THPC hydrogel (black), unloaded (blue) and loaded Fmoc-Met-OH hydrogels (red, dotted), and the composite material (green) after complete polymerization. Error bars represent standard deviations of experiments conducted in triplicates.

BSA/THPC hydrogel (Figure 2B) showed a smooth, even surface with small pores with an average pore diameter of 66 ± 7 nm (investigated by FIJI software[28]), explaining its rigidity and stability in the rheological analysis. In contrast, a branched fibrillary structure typical for Fmoc amino acid-based hydrogels[20] was found for the Fmoc-Met-OH layer building an architecture with cavities orders of magnitudes larger compared to those of the BSA/THPC hydrogel layer (Figure 2C). The larger cavities may already be sufficient to explain the different mechanical properties including the low-storage modulus of the Fmoc-Met-OH layer since pore sizes have a significant impact on the stability of hydrogels.[29] In summary, the BSA/THPC hydrogel, which was later used for the decoration with lectin as affinity or adapter molecules to mediate yeast-binding properties to the hydrogel surface, additionally provides an increase of stability to the fibrillary hydrogel, making it easier to handle. The two-layer hydrogel remained stable without rupture even after bending to 180° (**Figure 3**A), suggesting it is suitable for application as a wound dressing, which has to withstand the impact of different forces upon human movement. The two-layer hydrogel also showed adhesive properties to pork skin and could be removed residue free. The zone of adhesion thereby also showed the positive moisturizing effect of the hydrogel (Figure 3B). Although the adhesive properties are beneficial for the wound dressing, a fixing bandage would be used in any case of a real wound treatment.

2.3. Diffusion Analysis

A crucially important feature of the two-layer sandwich hydrogel is its ability to store and release drug molecules

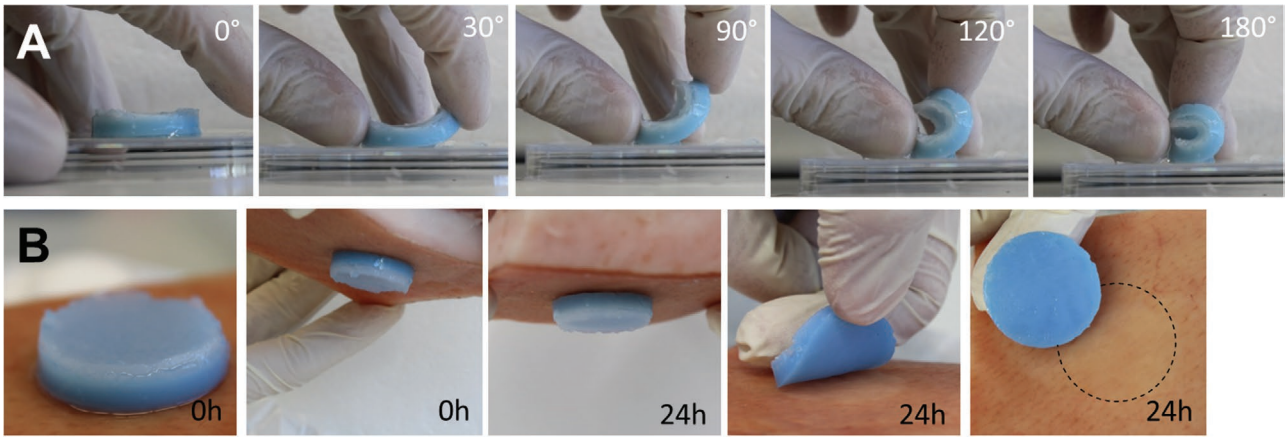

Figure 3. Flexibility and adhesion of the multicomponent hydrogel. The carrier layer was stained with bromophenol blue for better visualization. A) Bending of a multicomponent hydrogel from 0° to 180°. B) Multicomponent hydrogel adhering to pork skin directly after application (0 h). Adhesion- and residue-free peeling off of the multicomponent hydrogel after 24 h. The dotted black circle indicates the area of application, which showed the moisturizing effect of the hydrogel.

from the fibrillary network serving as a reservoir for releasing molecules into the protein hydrogel and into the environment (i.e., an infected wound). Therefore the carrier hydrogel was prepared in a 3D printed casting mold (**Figure 4**A). The resulting cavities were filled with the Fmoc-Met-OH hydrogel to generate drug reservoir gel inlays in the material (Figure 4B). The diffusion within the carrier layer was investigated with a rhodamine B-loaded reservoir, as amphiphilic model chemical compound.[12,30] Confocal laser scanning microscopy revealed an even distribution of rhodamine B in the BSA/THPC hydrogel after manufacturing and loading (Figure 4C). Quantitative analysis of fluorescence within the BSA/THPC hydrogel thereby reveals the penetration of the carrier layer from the reservoir layer at a rate of 2.35% min^{-1} until an equilibrium is reached 60 min after loading (Figure 4D). This fast and even distribution during the fabrication process of the two-layer sandwich hydrogel system is important for later industrial production processes. This easy loading ensures a homogeneously drug preloaded affinity layer with instant pharmacological effect for a convenient topical application of the wound dressing material.

The release from the wound dressing material was investigated in the two-layer hydrogel system, in which several carrier layers were tested with different BSA concentrations. The release reaches individual equilibria for the different gel concentrations (Figure 4E), suggesting that the release can be controlled by the BSA concentration used. However, all hydrogels showed a burst release within 5 h independent from the BSA concentration used (Figure 4F). Since the overall hardness of the composite material mainly depends on the elastic properties of the carrier layer (Figure 2F) and thus on the BSA concentration.[29,31] This promises that the mechanical properties of the intended final wound dressing can be tuned, without disturbing the burst release of an encapsulated drug, necessary for a convenient fast active treatment. The release rate of the 10% BSA hydrogel as a prototype reached its maximum within the first 2 h (Figure 4G), resulting in an almost complete release of the compound. In addition to the mentioned mechanical tunability, its capability for immediate delivery of antimicrobial drugs qualifies the composite as a potent material since immediate clearing of pathogens from infected wounds appears to be most critical after changing the surgical dressing to minimize the risk of deadly systemic infections for the patient.

2.4. Immobilization of Pathogenic Yeast Cells

The immobilization of pathogens within the hydrogel material was accomplished via a recombinant fusion between lectin and yellow fluorescent protein (YFP) as a reporter protein domain.[15] The purified YFP-LecB fusion protein was fully functional in binding *C. auris* and thus labeling the cells for fluorescence microscopy (**Figure 5**A). The BSA/THPC hydrogel, whose properties can easily be tailored and which has been shown to be biocompatible,[29,31] was decorated with recombinant YFP-LecB by chemical cross-linking[15] using bismaleimideoethane with fluorescence signals of the labeled material linear increasing with YFP-LecB concentrations and resulting in homogenous functionalization of the material (Figure 5B). The increasing YFP-LecB coverage was almost identical with an increase of binding capacity of the YFP-LecB hydrogel for *C. auris* reaching a complete coverage of approximately 90 000 cells mm^{-2} at lectin concentrations of 300×10^{-9} M, which is in accordance with the calculated value for the maximal coverage of 90 000 cells mm^2 taking an average yeast diameter of 3–4 µm into account[4] (Figure 5C,D). These findings constitute conclusive evidence that the BSA/THPC hydrogel layer can be decorated with YFP-LecB, which in turn binds and thus captures *C. auris* by the binding of carbohydrates on the surface of the cells.[32,33]

Based on cell density measurements, the minimal inhibitory concentration (MIC) was derived from a Lambert–Pearson plot[34] and found to be 11 µg of Cm-p5 per milliliter (**Figure 6**A), which is in a similar range as observed for other *Candida* species previously.[12] Cm-p5 also remained active in samples containing increasing concentrations of human blood serum incubated for 6 or 12 h, despite a nonsignificant decrease at 75% v/v blood serum (Figure 6B). Although wound exudate contains less proteins than blood serum, proteases are

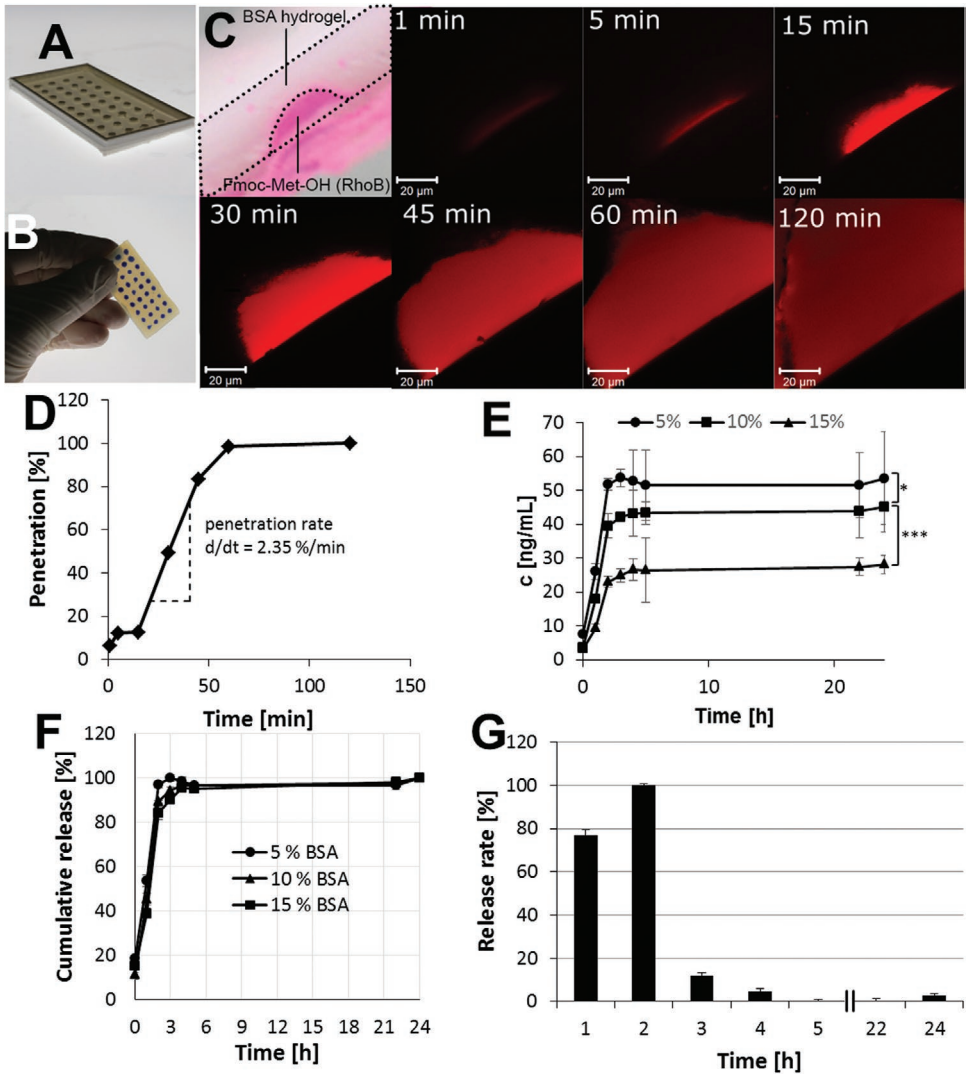

Figure 4. Characterization of diffusion within and from composite materials. A) 3D printed mold for the preparation of a composite material. B) BSA/THPC-hydrogel patch prepared in the mold containing Fmoc-Met-OH gel inlays. Fmoc-Met-OH gels were stained with bromophenol blue for better visualization. C) Time course of rhodamine B diffusion from the Fmoc-Met-OH inlays into the surrounding BSA/THPC-hydrogel visualized by confocal laser scanning microscopy (carrier layer penetration). D) Quantitative analysis of C) by FIJI software (version 1.51d). E) Release of rhodamine B from BSA/THPC-FmocMet-OH composite material depending on the BSA concentration (5%, 10%, or 15% w/v BSA) of the carrier layer. F) Cumulative release of rhodamine B from the composite material with different BSA concentrations in the carrier layer relative to the reached equilibrium concentration. G) Release rate ($\Delta c/\Delta t$) of the 10% BSA containing composite material calculated from panel (E).

also present in significant amounts[35] qualifying blood serum as a not ideal but reasonable substitute model.

To further prove the concept of a time-dependent and quantitative release of Cm-p5 from the Fmoc-Met-OH reservoir gel, while maintaining its functional integrity (i.e., toxicity toward *C. auris* cells), the toxicity toward *C. auris* was examined using Cm-p5 that was released from the gel after different periods, representing a simple readout for activity (i.e., maintenance of integrity) and concentration of the released peptide. Already after 8 h, the diffusion of the peptide from the gel into the collected sample buffer approached the equilibrium at 9 µg mL^{-1} that was sufficient to eliminate ≈80% of the *C. auris* cells in these experiments in solution, proving that Cm-p5 can be stored in the reservoir hydrogel layer and efficiently be quantitatively released from it into the environment in its active form (Figure 6C). The complete sandwich of both the Cm-p5 reservoir gel and the yeast affinity protein hydrogel was combined and its binding and killing functionality toward *C. auris* was proved in binding experiments to the final material and subsequent analysis using a microscopic assay based on resazurin to distinguish live from dead cells, since resazurin is exclusively metabolized to the fluorescent resorufin by living cells.[36] When loaded with Cm-p5, the sandwich hydrogel was able to significantly reduce the living *C. auris* cells even at concentrations below its MIC with 9×10^6 CFU at 10 µg mL^{-1} and no detectable colony formation at 80 µg mL^{-1} compared to 1.3×10^8 CFU mL^{-1} measured for the unloaded gel by the Miles and Misra method.[37] (Figure 6D,E).

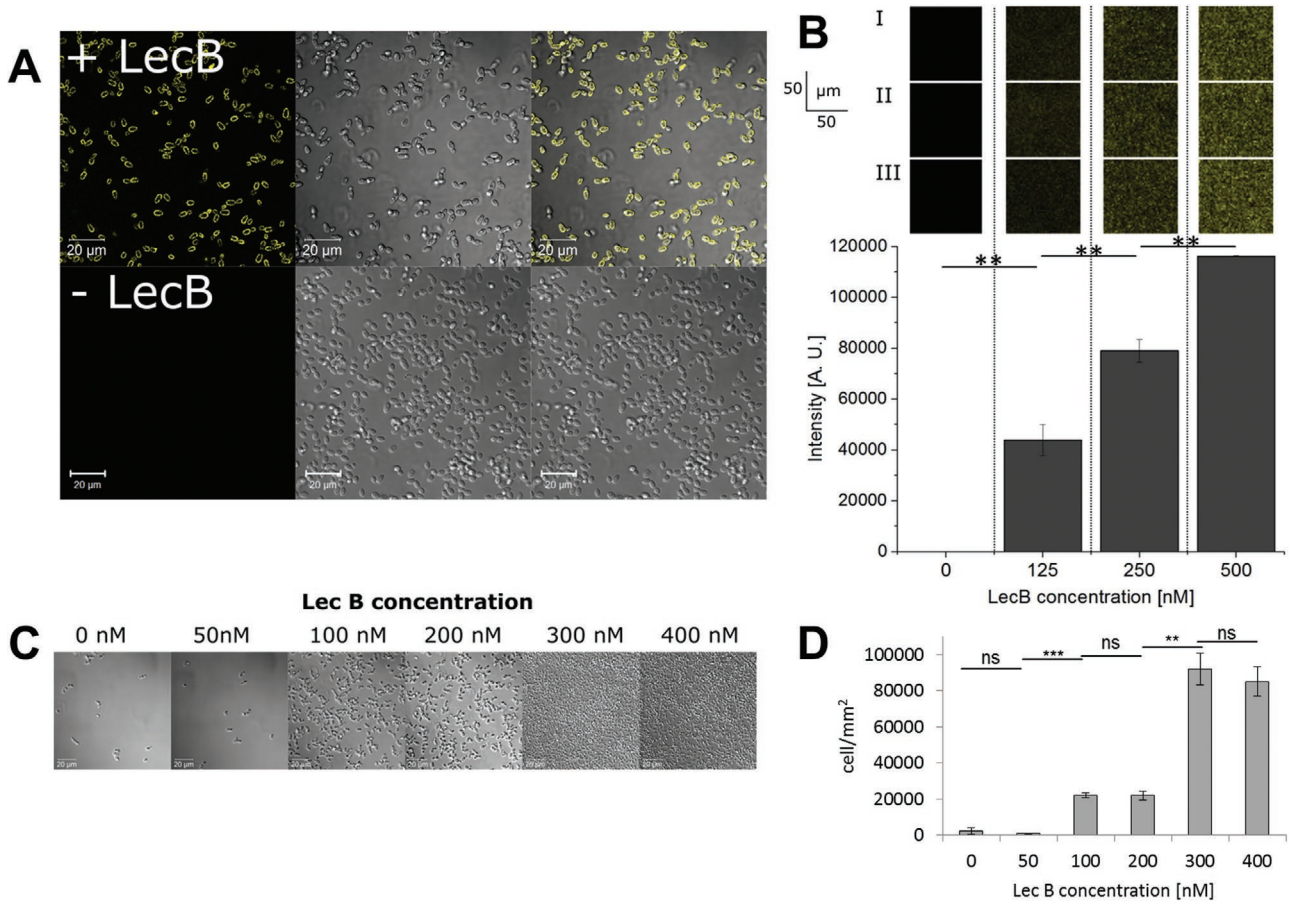

Figure 5. Lectin B used for the binding of *C. auris* and for the decoration of BSA/THPC hydrogels for subsequent yeast immobilization. A) YFP-LecB binding to *C. auris* cells visualized by confocal laser scanning microscopy at an excitation wavelength of 514 nm. B) Functionalization of the affinity hydrogel with recombinant-purified YFP-LecB fusion protein at different concentrations for 2 h at 21 °C using 10×10^{-3} M bismaleimideoethane as a cross-linker. Gels were analyzed by CLSM at an excitation of 514 nm. Representative 50 × 50 µm areas (I, II, and III) were converted in 32-bit grayscale and fluorescence was quantified by FIJI software (version 1.51d). C) Binding of *C. auris* to affinity hydrogels, functionalized with increasing amounts of YFP-LecB as affinity and imaging molecule. Bound cells were visualized by light microscopy. D) Surface coverage of the affinity layer counted by FIJI software from panel (C).

The final goal of our concept is the application of the hydrogel composites for wound care applications in which the establishment of severe and persisting infections is prohibited by removal of *C. auris* cells from the wound surface immediately after infection and subsequent killing of the pathogen. As a first and simple experimental step to approach this goal, a model surface consisting of collagen was used to mimic a naturally occurring extracellular matrix for cell binding, on which the two-layer hydrogel system could be directly applied. In confocal laser scanning microscopy, *C. auris* appeared completely viable, when grown on the collagen without any hydrogel treatment (**Figure 7**A). In comparison *C. auris* cells from surface that was facing the two-layer sandwich hydrogel but without direct contact were significantly impaired (Figure 7B), suggesting that Cm-p5 was released from the BSA layer into the moist collagen surface and could thus also act on cells in close proximity to the application site. In contrast, cells with direct contact to the two-layer sandwich hydrogel were completely eradicated by its antifungal properties (Figure 7C).

3. Conclusion

In only one decade since its first isolation, the threat of *C. auris* infections has become ubiquitous in clinical environments and it is developing alarmingly due to newly described transmission between patients and spreading on surfaces in clinical environments.[5] Yeast cells can enter the bloodstream causing fatal infections.[2] Prevention of such invasion through wounds is crucial already in early stages of surgical care and—in the case of multidrug-resistant pathogens such as *C. auris*—efficient and safe alternative drugs and novel concepts for their applications are urgently needed. We have reported the preparation and application of a functional two-layer hydrogels providing various important features that enable their usage as surgical dressings: The bilayer hydrogels exhibit an attractive stability, functionalization with bioactive peptides and proteins within each layer and diffusion characteristics, suitable for clinical wound care applications. Within few hours, an even distribution from the Fmoc-Met-OH into the BSA/THPC hydrogel layer was observed.

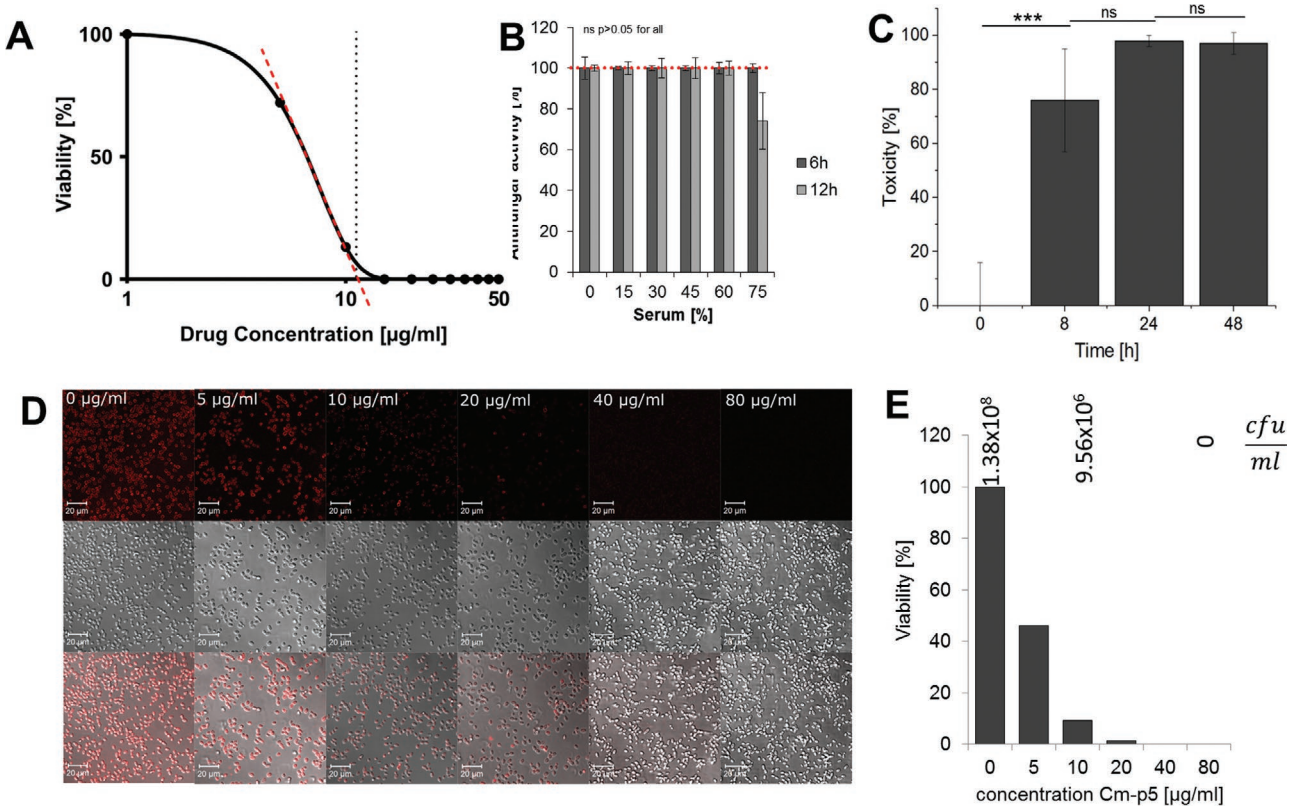

Figure 6. Antifungal activity of the peptide Cm-p5 against *C. auris*. A) The MIC determined by the broth microdilution method according to Clinical and Laboratory Standards Institute guidelines M27-A3 with additional spectrophotometrical measurements of the (optical) cell densities at 600 nm after 24 h illustrated as Lambert–Pearson plot. B) Antifungal activity of Cm-p5 remained stable after incubation for 6 h, respectively, 12 h in different human blood serum concentrations. For the sake of clear illustration, all the marks for nonsignificance have been excluded and only the mentioned significance has been included. C) Release of the antifungal peptide Cm-p5 from a fibrillary 0.8% w/v Fmoc-Met-OH hydrogel loaded with peptide. Solid gels were overlaid with equal volumes of PBS and the supernatant was collected after given periods. Antifungal effects of Cm-p5 released from gels were analyzed by the Miles and Misra method. D) Elimination of *C. auris* bound to the sandwich hydrogel functionalized with 400×10^{-9} M YFP-LecB. Hydrogels were incubated with *C. auris* suspensions with 2×10^5 cells. After washing with PBS, cell viability was monitored measuring the conversion of resazurin to fluorescent resorufin by living cells by CLSM at an excitation wavelength of 561 nm. E) Fluorescence and thus the amount of living cells were quantified from a 32-bit greyscale image of the detected signal by FIJI software (version 1.51d). Viability was further monitored by Miles and Misra Method.

Consequently, for a two-layer sandwich hydrogel prepared for clinical application, the BSA/THPC layer would be ready for an immediate drug release, while the Fmoc-Met-OH layer would further provide a reservoir for the anti-infective agent. The BSA/THPC layer further significantly reduced the loading of the pathogen *C. auris* by selective cell capturing within the affinity layer of the gel followed by subsequent AMP-dependent inactivation within the therapeutic Fmoc-Met-OH gel layer. In summary, this system paves the way for the topical treatment of multidrug-resistant *C. auris* species in medical wound care while keeping the load on the patient at a very low level.

Consequently, our results provide new avenues to protect patients from invasion by *C. auris* from infected wounds. Noteworthy, our platform technology could also be extended to other anti-infective agents. For instance, the AMP Cm-p5 has shown activity against *C. auris* and thus represents a very promising lead structure to identify next-generation drugs also against other *Candida* infections. We believe that local application of such bilayer affinity hydrogels provides a valuable strategy to overcome contaminations and spreading of pathogens, which is a key concern in surgical environments.

4. Experimental Section

Fabrication of the Two-Layer Sandwich Hydrogel: The carrier hydrogel was obtained by mixing a 20% BSA solution in PBS with an equal volume of a 3.57 mg mL^{-1} THPC solution (Sigma-Aldrich, Steinheim am Albuch, Germany). The Fmoc-Met-OH hydrogel on the other hand was prepared by spontaneous fibril formation by self-assembly upon mixing a 100 mg mL^{-1} Fmoc-Met-OH solution in DMSO with PBS containing the desired concentrations of Cm-p5 as an AMP at a ratio of 1:8.[20,22] The sandwich resulting from these two different hydrogels can simply be formed by either precasting the Fmoc-Met-OH hydrogel and overlaying it with the protein hydrogel or vice versa mediated by its self-adhesive properties.

The affinity layer was generated by overlaying the carrier layer hydrogel with a 10×10^{-3} M bismaleimideoethane (Thermo Fisher Scientific, Waltham, MA, USA) solution in PBS for 16 h, two washing steps with PBS, and addition of recombinant purified YFP-LecB fusion protein[15] at different concentrations for 2 h at 21 °C. After a final washing step,

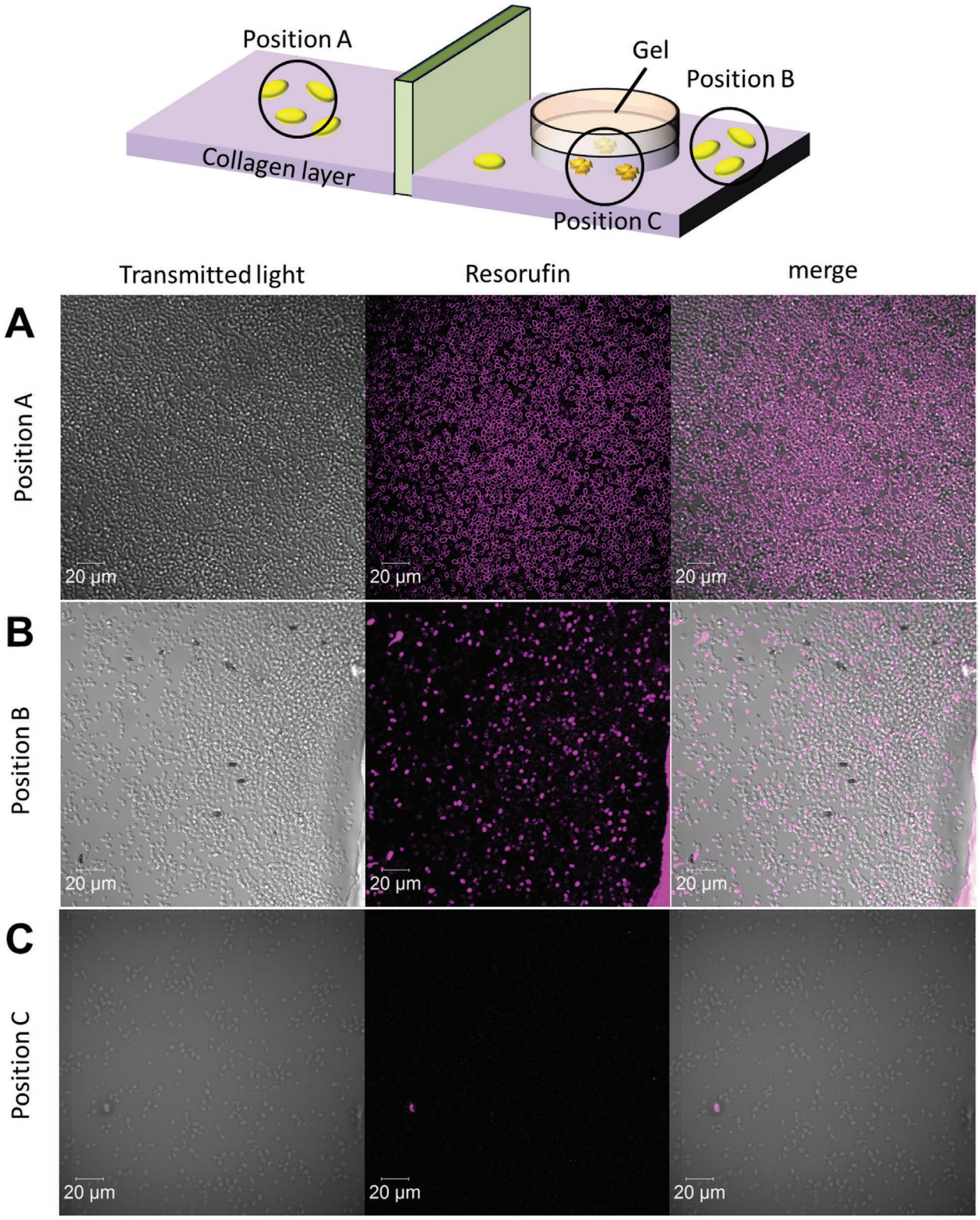

Figure 7. Killing of *C. auris* on a collagen-based surface with respect to its spatial distribution relative to the composite hydrogel. *C. auris* cells were applied on a collagen-based layer mimicking extracellular matrix exposed in a wound after injury. The BSA/THPC-Fmoc-Met-OH composite hydrogel loaded with Cmp5 (12 µg mL^{-1}) was applied directly onto the yeast with the BSA/THPC surface facing toward the collagen. Viability of *C. auris* was visualized using a resazurin live/dead assay and confocal laser scanning microscopy of fluorescent living cells. A) Living *C. auris* cells without any contact to the composite hydrogel (negative control). B) *C. auris* cells beneath but without direct contact to the composite hydrogel. C) *C. auris* cells directly under and with close contact to the composite hydrogel show no viability after 4 h.

gels were analyzed by controlled low strength material (CLSM) at an excitation of 514 nm. Representative 50 × 50 µm areas (I, II, and III) were converted in 32-bit grayscale and fluorescence was quantified by FIJI software (version 1.51d).[28]

Rheometry: The rheological properties of the two-layer hybrid hydrogel were investigated on a Kinexus Pro rotational rheometer (Malvern, Malvern, Worcestershire, UK) with a parallel plate geometry in triplicates. The gelation time of the Fmoc-Met-OH and the BSA/THPC-hydrogel was monitored by measuring the increase of the elastic shear modulus at a defined strain of 1% at 25 °C and a frequency of 0.1 Hz. The characterization of the final sandwich hydrogel system toward mechanical stress was, therefore, performed with gels after 16 h cross-linking to guarantee completion of the carrier hydrogel formation as the limiting step in the production of the fully functional biomaterial. Subsequently, the mechanical stability of single gel layers and the complete composite gels was measured upon submission to an oscillatory strain up to 300% and a preload of 0.2 N using pregelled gels. The frequency was thereby kept constant at 1 Hz and the temperature at 25 °C.

Electron Microscopy: The hydrogels were analyzed by cryo scanning electron microscopy, as described previously.[23] In short, the composite material was incubated in 30% isopropanol for 1 h. To preserve the native structure, samples from each layer were excised from the composite material, transferred to low-mass aluminum planchettes, and frozen under high pressure (Engineering Office M. Wohlwend GmbH, Sennwald, Switzerland). The gels were then transferred into a freeze etching device (BAF300, Bal-Tec, Principality of Lichtenstein) and dried at –90 °C for 30 min and subsequently coated with a 3 mm platinum layer. Analysis was performed with a cryo-stage Gatan 626 (Gatan-Inc., Pleasanton, California, USA) at a temperature of –100 °C and an acceleration voltage of 10 kV.

Adhesion Test: The adhesion of the final composite material was tested on pork skin obtained from a local butcher (EDEKA Center Ulm-Lehr, Ulm, Germany).

Diffusion Analysis: For the analysis of diffusion within the hydrogel system, a casting mold was modeled with the 3D modeling software SketchUp (Trimble Navigation Ltd., Sunnyvale, CA, USA) and 3D printed with a Wanhao Duplicator I3 (Wanhao, Jinhua, China) using polylactic acid filaments (Prima Filaments, Malmö, Sweden). A BSA/THPC hydrogel was then cast into this template and cross-linked. The resulting cavities within the BSA/THPC hydrogel were then filled with the Fmoc-Met-OH hydrogel. The diffusion in such a patch could be easily monitored by loading the Fmoc-Met-OH gel with 1 µg mL^{-1} rhodamine B as amphiphilic model chemical compound.[12,30] For the analysis of rhodamine B release from the two-layer sandwich hydrogel, the hydrogel system was overlayed with 2 mL PBS. The 2 mL Fmoc-Met-OH layer was again loaded with 1 µg mL^{-1} rhodamine and had a 1 mL BSA/THPC layer with a final BSA concentration of 5%, 10%, and 15%. The release was then monitored by measuring the increase of fluorescence in the supernatant with a Tecan Infinite M200 (Tecan Group, Männedorf, Switzerland) at an excitation wavelength of 535 nm and a emission wavelength of 595 nm. Concentrations were determined by a standard curve of different rhodamine B concentrations and illustrated as the cumulative release of the individual composite hydrogels relative to their reached equilibrium concentration.

The release rate was defined as the time-dependent increase of rhodamine B concentration in the supernatant ($\Delta c/\Delta t$) and was further determined only for the further used 10% BSA/THPC hydrogel.

Synthesis of Cm-p5: The antifungal peptide Cm-p5 was synthesized by the solid-phase method using 9-fluorenyl-methoxycarbonyl chemistry and purified by reverse phase high performance liquid chromatography to 98% purity using an acetonitrile/H_2O-TFA gradient. Purity was confirmed by ion spray mass spectrometry (Micromass, Manchester, UK).[12]

C. auris Growth and MIC Determination: *C. auris* (DSMZ-No. 21092, CBS 10913, JCM 15448)[1] was grown in YPD medium (1% w/v yeast extract, 2% w/v peptone, 2% w/v glucose) at 37 °C with orbital shaking at 150 rpm. Minimal inhibitory concentration assays were performed in RPMI-1640 medium supplemented with L-glutamine (Thermo Fisher Scientific, Waltham, MA, USA) according to the broth microdilution method of the Clinical and Laboratory Standards Institute guidelines M27-A3 with additional spectrophotometrical measurements of the (optical) cell densities at 600 nm after 24 h and MIC determination by a Lambert–Pearson plot.[34,38]

LecB Binding to C. auris: The immobilization of pathogens within the hydrogel material was accomplished via a recombinant fusion between lectin and YFP as a reporter protein domain.[15] Its binding toward *C. auris* was tested by incubating 2 × 10^3 (standardized in 20 µL) cells in a 250 × 10^{-9} M YFP-LecB solution, washing in PBS (2.6 × 10^{-3} M KCl, 1.5 × 10^{-3} M KH_2PO_4, 8 × 10^{-3} M Na_2HPO_4, 137 × 10^{-3} M NaCl, pH 7), and subsequent visualization by confocal laser scanning microscopy.

Immobilization of C. auris: Binding of *C. auris* cells to the affinity layer, functionalized with different concentrations (0–400 × 10^{-9} M) of YFP-LecB as a binding and imaging molecule, was investigated by the addition of 200 µL cell suspension (10^6 cells mL^{-1}) and incubation for 60 min at 21 °C. After washing twice with 100 µL PBS, bound cells were observed by light microscopy.

Stability of Cm-p5 in Human Blood Serum: Cm-p5 (40 µg mL^{-1}) was incubated at 25 °C with increasing amounts of human AB serum (Sigma-Aldrich, St. Louis, Missouri, USA). After 6 h, respectively, 12 h *C. auris* in RPMI-1640 medium was added to a final cell number of 2 × 10^3 (final Cm-p5 concentration 20 µg mL^{-1}) and incubated for 24 h at 37 °C. The activity of Cm-p5 was determined from the growth of *C. auris* relative to the growth in human serum containing medium in the absence of Cm-p5.

Antifungal Activity of Cm-p5 Released from Hydrogels: Fmoc-Met-OH (Carl Roth GmbH & Co. KG, Karlsruhe, Germany) 10% w/v dissolved in DMSO and Cm-p5 (1.5 mg mL^{-1} in DMSO) were added to PBS to a final Fmoc-Met-OH concentration of 0.8% w/v and a peptide concentration of 80 µg mL^{-1}. Solid gels were overlaid with equal volumes of PBS and the supernatant was collected after given periods. Antifungal effects of Cm-p5 released from gels were analyzed by the Miles and Misra method.[37] The final composite hydrogel sandwich was obtained by casting BSA hydrogels on top of Cm-p5 Fmoc-Met-OH hydrogel reservoirs (concentrations 0–80 µg mL^{-1}) and functionalized with 400 × 10^{-9} M YFP-LecB. These hydrogels were incubated with *C. auris* suspensions with 2 × 10^5 cells in 200 µL for 2 h at 21 °C. After washing with PBS, the sandwich hydrogels were incubated with 0.1 mg mL^{-1} resazurin (Sigma-Aldrich) for 1 h at 21 °C, cells were washed with PBS, and cell viability was monitored measuring the conversion of resazurin to fluorescent resorufin by living cells by CLSM at an excitation wavelength of 561 nm. The fluorescence and thus the amount of living cells were quantified from a 32-bit grayscale image of the detected signal by FIJI software (version 1.51d). Additionally, viability was also investigated by the Miles and Misra method after releasing bound cells from the affinity layer with 200 µL 20 × 10^{-3} M mannose in PBS.

Collagen Surface Substrate Model: A model for wound care application was composed of collagen, which was gelated by mixing 150 µL of 1 mg mL^{-1} stock solution of collagen from rat tail in PBS with 1.5 µL of 1 M NaOH in eight-well Ibidi µ-Slide (ibidi, Martinsried, Germany). Gelation was performed for 1 h at 30 °C. To expose this layer toward the yeast, 200 µL of a *C. auris* culture in YPD medium[39] containing 2 × 10^5 *C. auris* cells was loaded onto the collagen surface. The composite hydrogel loaded with Cm-p5 (12 µg mL^{-1}) was placed on top of the collagen layer by transferring it from the casting mold with tweezers with the affinity layer facing the cells. After 2 h, 10 µL of a sterile 0.1% resazurin solution were added to the *C. auris* cells. The viability of *C. auris* was analyzed by confocal laser scanning microscopy after 2 h at 561 nm, as described before, with respect to the position of the cells in this artificial wound immediately beneath or in close contact to the antifungal wound dressing.

Statistical Analysis: Statistical analysis was performed by a paired *t*-test.

Acknowledgements

C.F. and H.R. contributed equally to this work. This work was supported by the in the framework of "Bioinspired Material Synthesis", the Ministry

of Science, Research and Arts of the state of Baden-Württemberg in the framework of the PhD program: pharmaceutical biotechnology, the Federal Ministry of Education and Research (BMBF-WTZ-DLR, Germany-Cuba, 2018–2020; BMBF/DLR 01DN18009; BMBF, Biotechnologie 2020+ Basistechnologien: Projekt SeleKoM), the European Union project "Horizon 2020" (No. 686271) in the framework "AD-gut," and the Collaborative Research Center (CRC1279).

Conflict of Interest

The authors declare no conflict of interest.

Keywords

Candida auris, compound encapsulation, drug delivery, intrinsic antimicrobial activity, multicomponent hydrogels

Received: January 7, 2020
Revised: February 7, 2020
Published online:

[1] K. Satoh, K. Makimura, Y. Hasumi, Y. Nishiyama, K. Uchida, H. Yamaguchi, *Microbiol. Immunol.* **2009**, *53*, 41.
[2] S. E. Morales-López, C. M. Parra-Giraldo, A. Ceballos-Garzón, H. P. Martínez, G. J. Rodríguez, C. A. Álvarez-Moreno, J. Y. Rodríguez, *Emerg. Infect. Dis.* **2017**, *23*, 162.
[3] S. R. Lockhart, K. A. Etienne, S. Vallabhaneni, J. Farooqi, A. Chowdhary, N. P. Govender, A. L. Colombo, B. Calvo, C. A. Cuomo, C. A. Desjardins, E. L. Berkow, M. Castanheira, R. E. Magobo, K. Jabeen, R. J. Asghar, J. F. Meis, B. Jackson, T. Chiller, A. P. Litvintseva, *Clin. Infect. Dis.* **2017**, *64*, 134.
[4] J. Osei Sekyere, *MicrobiologyOpen* **2018**, *7*, e00578.
[5] C. T. Piedrahita, J. L. Cadnum, A. L. Jencson, A. A. Shaikh, M. A. Ghannoum, C. J. Donskey, *Infect. Control Hosp. Epidemiol.* **2017**, *38*, 1107.
[6] Centers for Disease Control and Prevention, Clinical Alert to U.S. Healthcare Facilities—June 2016—Fungal Diseases **2016**, https://www.cdc.gov/fungal/candida-auris/candida-auris-alert.html (accessed: February 2020).
[7] Forbes, https://www.forbes.com/sites/judystone/2017/08/24/candida-auris-a-new-fungal-superbug-emerging-as-a-global-threat/, (accessed: August 2018).
[8] T. Ciociola, L. Giovati, S. Conti, W. Magliani, C. Santinoli, L. Polonelli, *Future Med. Chem.* **2016**, *8*, 1413.
[9] M. Rautenbach, A. M. Troskie, J. A. Vosloo, *Biochimie* **2016**, *130*, 132.
[10] A. Hollmann, M. Martinez, P. Maturana, L. C. Semorile, P. C. Maffia, *Front. Chem.* **2018**, *6*, 204.
[11] F. E. M. Vicente, M. González-Garcia, E. Diaz Pico, E. Moreno-Castillo, H. E. Garay, P. E. Rosi, A. M. Jimenez, J. A. Campos-Delgado, D. G. Rivera, G. Chinea, R. C. L. R. Pietro, S. Stenger, B. Spellerberg, D. Kubiczek, N. Bodenberger, S. Dietz, F. Rosenau, M. W. Paixão, L. Ständker, A. J. Otero-González, *ACS Omega* **2019**, *4*, 19081.
[12] C. López-Abarrategui, C. McBeth, S. M. Mandal, Z. J. Sun, G. Heffron, A. Alba-Menéndez, L. Migliolo, O. Reyes-Acosta, M. García-Villarino, D. O. Nolasco, R. Falcão, M. D. Cherobim, S. C. Dias, W. Brandt, L. Wessjohann, M. Starnbach, O. L. Franco, A. J. Otero-González, *FASEB J.* **2015**, *29*, 3315.
[13] A. Francesko, P. Petkova, T. Tzanov, *Curr. Med. Chem.* **2017**.
[14] E. A. Kamoun, E. R. S. Kenawy, X. Chen, *J. Adv. Res.* **2017**, *8*, 217.
[15] N. Bodenberger, D. Kubiczek, D. Halbgebauer, V. Rimola, S. Wiese, D. Mayer, A. A. Rodríguez Alfonso, S. Stenger, F. Rosenau, *Biomacromolecules* **2018**, *19*, 2472.
[16] A. Khan, M. Xu, T. Wang, C. You, X. Wang, H. Ren, H. Zhou, A. Khan, C. Han, P. Li, *Biosci. Rep.* **2019**, *39*, BSR20190504.
[17] G. Yang, T. Huang, Y. Wang, H. Wang, Y. Li, K. Yu, L. Dong, *J. Biomater. Sci., Polym. Ed.* **2018**, *29*, 1812.
[18] N. Bodenberger, D. Kubiczek, L. Trösch, A. Gawanbacht, S. Wilhelm, D. Tielker, F. Rosenau, *Sci. Rep.* **2017**, *7*.
[19] D. Tielker, F. Rosenau, K. M. Bartels, T. Rosenbaum, K. E. Jaeger, *BioTechniques* **2006**, *41*, 327.
[20] E. R. Draper, K. L. Morris, M. A. Little, J. Raeburn, C. Colquhoun, E. R. Cross, T. O. McDonald, L. C. Serpell, D. J. Adams, *CrystEngComm* **2015**, *17*, 8047.
[21] S. Atefyekta, M. Pihl, C. Lindsay, S. C. Heilshorn, M. Andersson, *Acta Biomater.* **2019**, *83*, 245.
[22] V. Singh, K. Snigdha, C. Singh, N. Sinha, A. K. Thakur, *Soft Matter* **2015**, *11*, 5353.
[23] S. Brien, P. Prescott, N. Bashir, H. Lewith, G. Lewith, *Osteoarthritis Cartilage* **2008**, *16*, 1277.
[24] C. Chung, K. J. Lampe, S. C. Heilshorn, *Biomacromolecules* **2012**, *13*, 3912.
[25] M. Fürsatz, M. Skog, P. Sivlér, E. Palm, C. Aronsson, A. Skallberg, G. Greczynski, H. Khalaf, T. Bengtsson, D. Aili, *Biomed. Mater.* **2018**, *13*, 025014.
[26] H. Joodaki, M. B. Panzer, *J. Eng. Med.* **2018**, *232*, 323.
[27] I. Levental, P. C. Georges, P. A. Janmey, *Soft Matter* **2007**, *3*, 299.
[28] J. Schindelin, I. Arganda-Carreras, E. Frise, V. Kaynig, M. Longair, T. Pietzsch, S. Preibisch, C. Rueden, S. Saalfeld, B. Schmid, J. Y. Tinevez, D. J. White, V. Hartenstein, K. Eliceiri, P. Tomancak, A. Cardona, *Nat. Methods* **2012**, *9*, 676.
[29] N. Bodenberger, P. Paul, D. Kubiczek, P. Walther, K. E. Gottschalk, F. Rosenau, *ChemistrySelect* **2016**, *1*, 1353.
[30] T. Osakai, H. Yamada, H. Nagatani, T. Sagara, *J. Phys. Chem. C* **2007**, *111*, 9480.
[31] N. Bodenberger, D. Kubiczek, I. Abrosimova, A. Scharm, F. Kipper, P. Walther, F. Rosenau, *Biotechnol. Rep.* **2016**, *12*, 6.
[32] N. Sharon, H. Lis, *Science* **1989**, *246*, 227.
[33] M. Monsigny, R. Mayer, A. C. Roche, *Carbohydr. Lett.* **2000**, *4*, 35.
[34] R. J. W. Lambert, J. Pearson, *J. Appl. Microbiol.* **2000**, *88*, 784.
[35] K. F. Cutting, *Br. J. Community Nurs.* **2003**, *8*, S4.
[36] T. L. Riss, R. A. Moravec, A. L. Niles, S. Duellman, H. A. Benink, T. J. Worzella, L. Minor, *Assay Guid. Man. Internet* **2013**, *114*, 785.
[37] A. A. Miles, S. S. Misra, J. O. Irwin, *J. Hyg.* **1938**, *38*, 732.
[38] CLSI, Reference method for broth dilution antifungal susceptibility testing of yeasts; approved standard, 3rd ed., CLSI, Wayne, PA **2008**.
[39] I. Corbacho, F. Teixidó, R. Velázquez, L. M. Hernández, I. Olivero, A. van Leeuwenhoek, *Int. J. Gen. Mol. Microbiol.* **2011**, *99*, 591.